Supramolecular Hemoprotein Assembly with a Periodic Structure Showing Heme–Heme Exciton Coupling

Koji Oohora,*[†‡§] Nishiki Fujimaki,[†] Ryota Kajihara,[†] Hiroki Watanabe,[‖] Takayuki Uchihashi,*[‖] Takashi Hayashi*[†]

[†] Department of Applied Chemistry, Graduate School of Engineering, Osaka University, Suita 565-0871, Japan
[‡] Frontier Research Base for Global Young Researchers, Graduate School of Engineering, Osaka University, Suita 565-0871, Japan
[§] PRESTO, Japan Science and Technology Agency (JST), Kawaguchi 332-0012, Japan
[‖] Department of Physics, Nagoya University, Nagoya, 464-8602, Japan

Materials and Methods

Instruments: ESI-TOF MS analyses were performed with a Bruker Daltonics micrOTOF II mass spectrometer. UV-vis spectra were measured with a Shimadzu BioSpec-nano or Shimadzu UV-3150 double-beam spectrometer. Circular dichroism (CD) spectra were recorded with a JASCO J-820S spectrometer. Size exclusion chromatographic (SEC) analyses were performed using a Superdex 200 10/300 GL (GE Healthcare) column with an ÄKTApurifier system (GE Healthcare) at 4 ºC. pH measurements were made with an F-52 Horiba pH meter.

Materials: Maleimide-tethered heme, **1**, was prepared according to procedures reported in the literature.[S1] Unless mentioned otherwise, all protein solutions were dissolved in a 100 mM potassium phosphate buffer, pH 7.0. Other reagents and chemicals were purchased and used as received. Distilled water was demineralized using a Barnstead NANOpure Diamond apparatus.

Protein Sequence of Cytochrome b_{562} Mutants

Cyt b_{562}
ADLEDNMETLNDNLKVIEKADNAAQVKDALTKMRAAALDAQKATPPKLEDKSPDSPEMK
DFRHGFDILVGQIDDALKLANEGKVKEAQAAAEQLKTTRNAYHQKYR
H63C
ADLEDNMETLNDNLKVIEKADNAAQVKDALTKMRAAALDAQKATPPKLEDKSPDSPEMK
DFRCGFDILVGQIDDALKLANEGKVKEAQAAAEQLKTTRNAYHQKYR
N80C
ADLEDNMETLNDNLKVIEKADNAAQVKDALTKMRAAALDAQKATPPKLEDKSPDSPEMK
DFRHGFDILVGQIDDALKLACEGKVKEAQAAAEQLKTTRNAYHQKYR
N80C/D73A
ADLEDNMETLNDNLKVIEKADNAAQVKDALTKMRAAALDAQKATPPKLEDKSPDSPEMK
DFRHGFDILVGQIADALKLACEGKVKEAQAAAEQLKTTRNAYHQKYR
N80C/R98A
ADLEDNMETLNDNLKVIEKADNAAQVKDALTKMRAAALDAQKATPPKLEDKSPDSPEMK
DFRHGFDILVGQIDDALKLACEGKVKEAQAAAEQLKTTANAYHQKYR

Preparation of Cytochrome b_{562} Mutants

The gene expression system for wild type cytochrome b_{562}, Cyt b_{562}, and its single mutant, H63C, were reported in our previous paper.[S2] To obtain the gene expression system for N80C mutant, site-directed mutagenesis was performed by the polymerase chain reaction (PCR) using the LA PCR *in vitro* Mutagenesis Kit (Takara) according to the protocol of the manufacturer. The Cyt b_{562} gene cloned into pUC118 was used as a template to introduce the N80C single mutation into the protein. The primer sequences used to generate N80C mutant are:
5'-GACGACGCGCTGAAGCTGGCATGCGAAGGTAAAGTAAAAGAAGCG-3' and the complementary primer.

After PCR, the template DNA plasmids were digested with Dpn I (Thermo Fisher Scientific). *E. coli* DH5α competent cells were transformed with the PCR products. After the cultivation, the plasmids were purified using the PureLink™ Quick Plasmid Miniprep Kit (Thermo Fisher Scientific). DNA sequencing was performed to verify each correct mutation in the gene sequence. The mutant protein was overexpressed in the *E. coli* strain TG-1 and purified using cation exchange and gelfiltration column chromatography as previously described.[S2] The obtained N80C mutant was characterized by SDS-PAGE and ESI-TOF MS, and stored at –80 °C.

The gene for expression of Cyt b_{562} double mutants, N80C/D73A and N80C/R98A, were prepared using the N80C gene as a template and the following primers with the above protocol.
N80C/D73A: 5'-GACATTCTGGTCGGTCAGATTGCGGACGCGCTGAAGCTGGCATGC-3' and the complementary primer.

N80C/R98A: 5'-GCAGAGCAACTGAAAACGACCGCGAACGCCTATCACCAGAAGTAT-3' and the complementary primer.

Surface Modification Reaction of Cytochrome b_{562} Mutants

Before the reaction, an N80C stock solution was treated by addition of 10 mM dithiothreitol to reduce disulfide bonds and purified using a HiTrap desalting column equilibrated with N_2-purged 50 mM Tris HCl buffer, pH 8.0 containing 0.1 mM EDTA. To an N80C solution (0.50 μmol 5.0 mL), a solution of **1** (2.6 μmol) in DMF (0.9 mL) was added under an N_2 atmosphere. After stirring in the dark for 3 h at room temperature, the solution was acidified by addition of 1 M aqueous HCl to pH 1.7 and then free heme was extracted with cooled 2-butanone. The solution was neutralized by dialysis using 100 mM potassium phosphate buffer, pH 7.0. The obtained **1**-N80C was characterized by ESI-TOF MS (Figure S1), and stored at –80 ˚C (Yield: 4.0 mg, 0.32 μmol, 64 %). Other monomers, **1**-H63C, **1**-N80C/D73A and **1**-N80C/R98A, were prepared according to the same procedures used for preparation of **1**-N80C. The protein surface modification was confirmed by ESI-TOF MS: **1**-N80C (found *m*/*z*: 1251.70, calcd *m*/*z* (*z* = 10+): 1251.75), **1**-H63C (found *m*/*z*: 1249.78 calcd *m*/*z* (z = 10+): 1249.58), **1**-N80C/D73A (found *m*/*z*: 1134.12, calcd *m*/*z* (*z* = 11+): 1134.04) and **1**-N80C/R98A (found *m*/*z*: 1036.13, calcd *m*/*z* (*z* = 12+): 1036.19).

SEC Analysis

For SEC analysis, 100 mM potassium phosphate buffer, pH 7.0, was used as an eluent. The analysis was performed with a flow rate of 0.5 mL/min at 4 ºC with monitoring of the absorbance at 418 nm and 280 nm for detection. The column was validated using the following reagents (Gel Filtration Calibration kits HMW and LMW, GE Healthcare): thymoglobulin (669 kDa), ferritin (440 kDa), catalase (232 kDa), albumin (67 kDa), ribonuclease A (13.7 kDa). In the analysis of the protein assembly, 200 μM of the samples as the monomer concentrations were used.

High-Speed Atomic Force Microscopy (HS-AFM) Imaging

HS-AFM imaging was carried out using a laboratory-designed HS-AFM apparatus in tapping-mode operation.[S3] The dimensions of the cantilever (Olympus) were 6−7 μm length, 2 μm width, and 90 nm thickness. The nominal spring constant was 0.1−0.2 N/m, the resonant frequency was 0.7−1 MHz, and the quality factor in aqueous solution was ca. 2. For HS-AFM imaging, the free oscillation amplitude was set to 1−2 nm, and the set-point amplitude was approximately 90% of the free oscillation amplitude. An amorphous carbon tip grown by electron-beam deposition with scanning electron microscopy was used.[S4] After the electron-beam deposition, the tip was sharpened by plasma etching under Ar gas (tip apex, d = ca. 4 nm).

In the HS-AFM imaging and processing, poly-L-lysine on mica (Phasis, Switzerland) or APTES ((3-Aminopropyl)triethoxysilane)-treated mica was used as a substrate. The solution (3 μL) of 0.02 μM **1**-N80C assembly was deposited onto the substrate. After the 3-min incubation, the substrate was thoroughly washed with a buffer (80 mM HEPES, NaOH pH 7.0) to remove excess molecules. The HS-AFM imaging was performed in the buffer at room temperature.

Molecular Dynamics (MD) Simulation

The modeling was performed using YASARA[S5] Structure Version 13.6.16 that employed force field AMBER03[S6] for protein residues and GAFF[S7] using AM1/BCC[S8] partial charges for the heme moiety covalently bound to Cys80. The calculation was carried out using YASARA Structure Version 13.6.16 employing force field AMBER03. To maintain the correct coordination geometry, the distances from the metal to all four pyrrole N atoms of the porphyrin ligand were constrained to 2.0 Å. The hexa-coordination by ligation with Met7 and His102 was represented by two force field arrows and the distances of the Fe–S and Fe–N dative bonds were constrained to 2.3 and 2.0 Å, respectively, according to the NMR structure (PDB ID: 1QPU) of Cyt b_{562}. The partial charge of the metal was set to +2 and the total charge of the heme was set to zero. For the dimer model, the four different models of isomers generated by the combination of two modification points of propionate side chains with two enantiomers by cysteine–maleimide linkage were designed as independent initial structures (models A-D as shown in Figures S2–S5). Each structure of the dimer model was solvated in a box of TIP3P water molecules using periodic boundaries at pH 7.0 and a density of 0.997 g/mL. Each pre-minimized structure was obtained by steepest descent minimization and simulated annealing, which was then relaxed using molecular dynamics calculations at 298 K over 225 ns and snapshots were taken at 250 ps intervals to analyze the heme–heme distances and dihedral angles (Figures S2–S5). The nonamer initial structure was manually constructed according to the suitable dimer model A. The modeled structure of the **1**-N80C nonamer was solvated in a box of TIP3P water molecules using periodic boundaries at pH 7.0 and a density of 0.997 g/mL. The preminimized structure was obtained by steepest descent minimization and simulated annealing, which was then relaxed using molecular dynamics calculations at 298 K for 10 ns and snapshots were taken at 250 ps intervals to analyze the heme-heme distances and dihedral angles.

Simulation of CD Spectra Using an Empirical Exciton Coupling Method

The simulation of CD spectra was carried out using the reported empirical exciton coupling method.[S9,S10] In this work, The exciton coupling energy, V_{ij}, between the transition dipole moments of two chromophores, $\boldsymbol{\mu}_i$ and $\boldsymbol{\mu}_j$, was calculated by

$$V_{ij} = \frac{\boldsymbol{\mu}_i \cdot \boldsymbol{\mu}_j}{(R_{ij})^3} - 3\frac{(\boldsymbol{\mu}_i \cdot \mathbf{R}_{ij})(\boldsymbol{\mu}_j \cdot \mathbf{R}_{ij})}{(R_{ij})^5} \qquad \text{eq 1}$$

where $\mathbf{R}_{ij}$ is the interchromophoric vector and $R_{ij} = |\mathbf{R}_{ij}|$. $\mathbf{R}_{ij}$ is obtained from the coordinates of iron centers of two heme moieties in the MD-minimized dimer model. The dipole length of $\boldsymbol{\mu}$ was determined to be 2.06 Å from the fitting peak for the Soret band of the experimental UV-vis spectrum using the Gauss function (Figure S6) and the unit vector of $\boldsymbol{\mu}$ was obtained from the coordinates of the dipole of the meso–meso positions in the porphyrin moieties (Figure S7, Tables S1-4). Using the V_{ij} values derived from the combination of each two transition moments in two heme moieties, the CD spectrum was simulated according to the reported empirical method.[S10] Here, we use following equations:

$$\sigma_k - \sigma_{\max} = 2\sum_{i=1}^{N}\sum_{j>i}^{N} C_{ik}C_{jk}V_{ij} \qquad \text{eq 2}$$

$$R_k = \pi\sigma_{max}\sum_{i=1}^{N}\sum_{j>1}^{N} C_{ik}C_{jk}R_{ij}\,\mu_i\mu_j\left(\boldsymbol{e_{ij}} \cdot \boldsymbol{e_j} \times \boldsymbol{e_i}\right) \qquad \text{eq 3}$$

$$\Delta\varepsilon(\sigma) = \frac{\sigma_0}{2.296\times10^{-39}\sqrt{\pi}\Delta\sigma}\sum_{k=1}^{N} R_k \exp\left[-\frac{(\sigma-\sigma_k)^2}{\Delta\sigma^2}\right] \qquad \text{eq 4}$$

where $\sigma_k - \sigma_{max}$, C, R_k and $\boldsymbol{e}$ are eigenvalue, eigenvector coefficient, rotational strength and unit vector of μ, respectively. The eq 3 is specific for coordinates in the left-handed system, which is default in YASARA software.

Simulation of AFM images

Simulation of AFM images was performed using custom software based on IgorPro 6 (Wavemetrics, Lake Oswego, Ore., USA) software. The pseudo AFM image was generated for a cone-shaped AFM tip with a radius of 0.5 nm and half cone angle of 10°, and the MD-simulated structure of the **1**-N80C nonamer. During the simulation, the orientation of the **1**-N80C nonamer was rotated along the longitudinal axis of the fibril and adjusted so that the appearance of the simulated image was close to the experimental AFM image. After construction of the simulated image, the image was filtered by a low-pass filter with a cut off spatial frequency of 2 nm because the spatial resolution of the HS-AFM is generally limited to 2 nm.

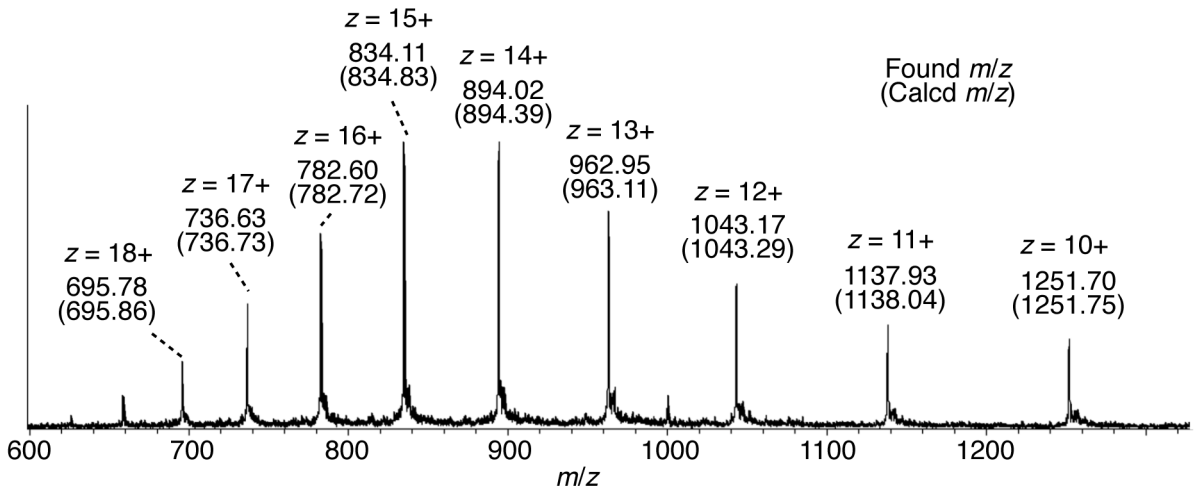

Figure S1. ESI- TOF MS for the characterization of **1**-N80C. The protein was dissolved in 50% acetonitrile aqueous solution containing 0.1% HCOOH.

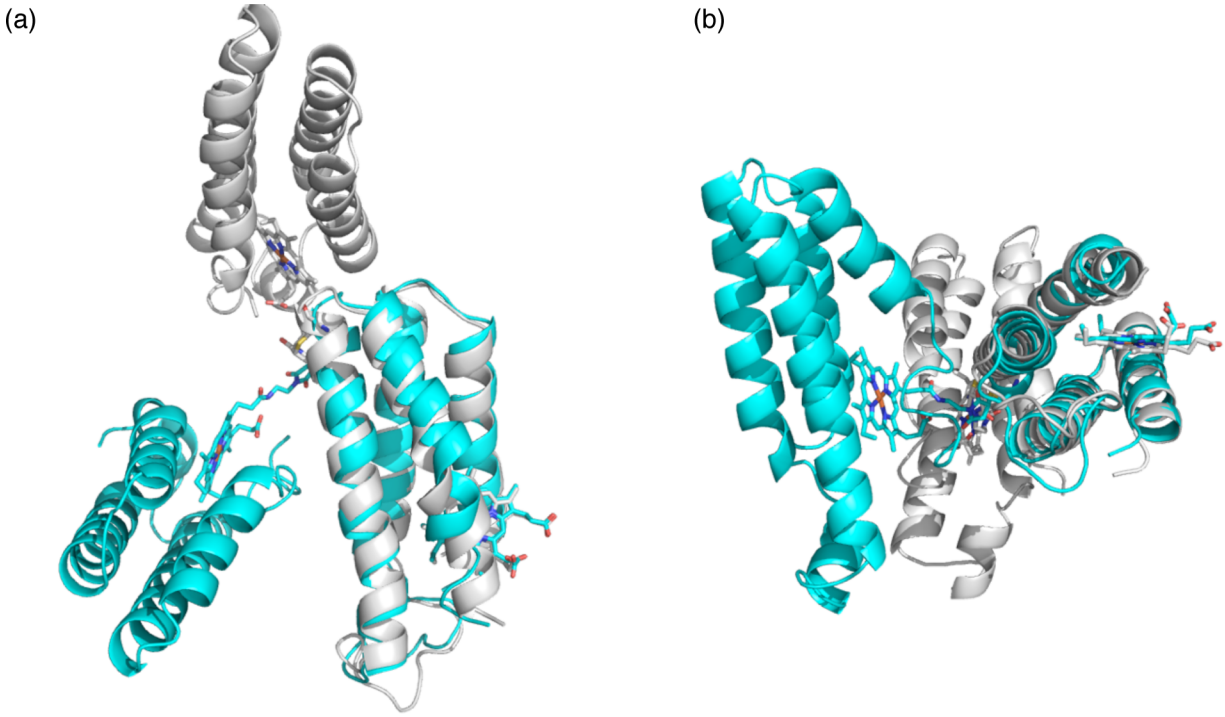

Figure S2. Dimer model A, which is discussed in the main text. The initial and MD-relaxed structures are shown in gray and cyan, respectively. The two structures are superimposed by Cα carbons of **1**-N80C with native heme. (a) Top view. (b) Side view.

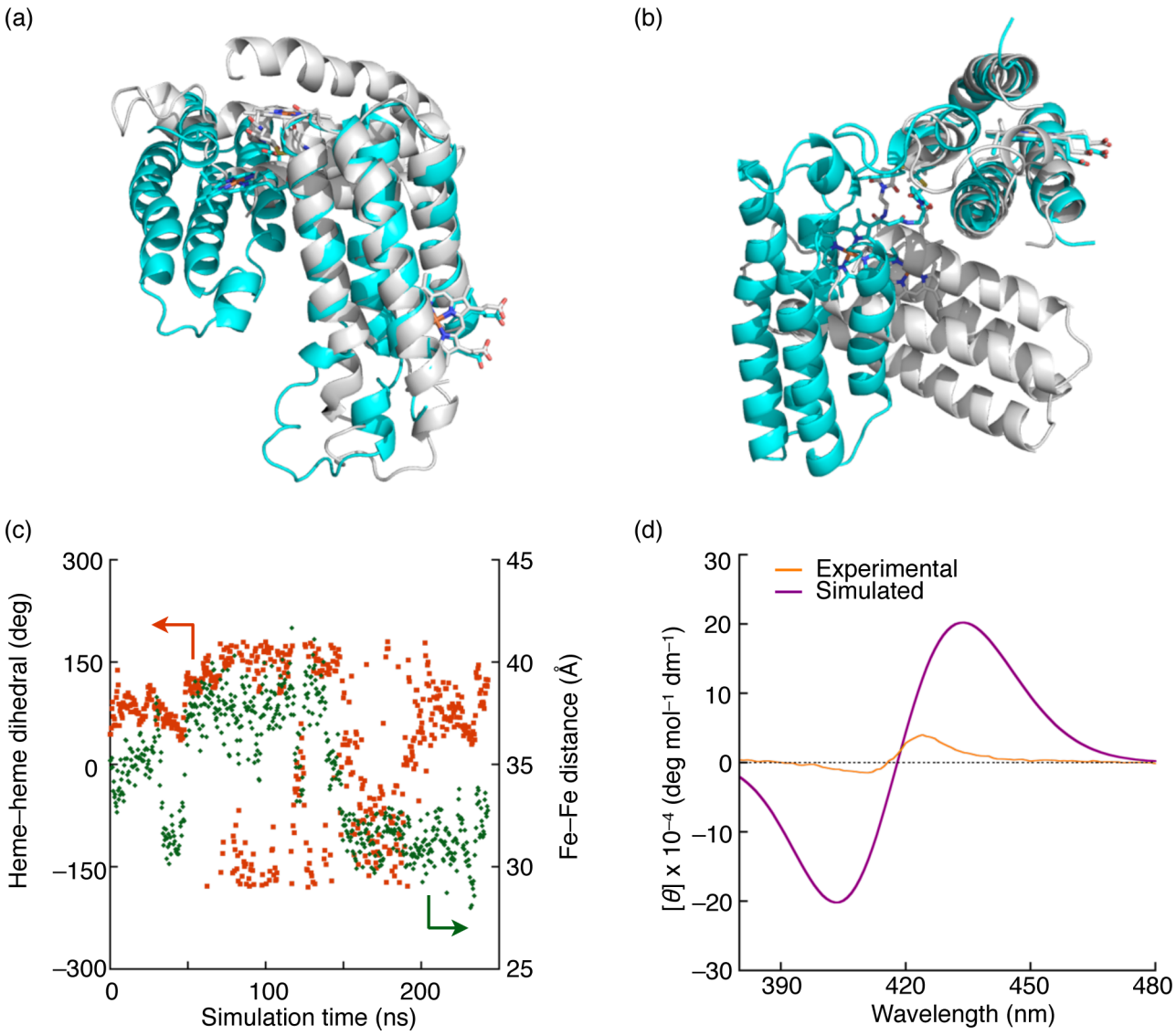

Figure S3. Dimer model B. The initial and MD-relaxed structures are shown in gray and cyan, respectively. The two structures are superimposed by Cα carbons of **1**-N80C with native heme. (a) Top view. (b) Side view. (c) The plots of important structural factors, heme–heme dihedral angles (red) and Fe–Fe distances (green), of the dimer model against the simulation time. (d) Simulated CD spectrum based on the model B (purple) and experimental CD spectrum (orange).

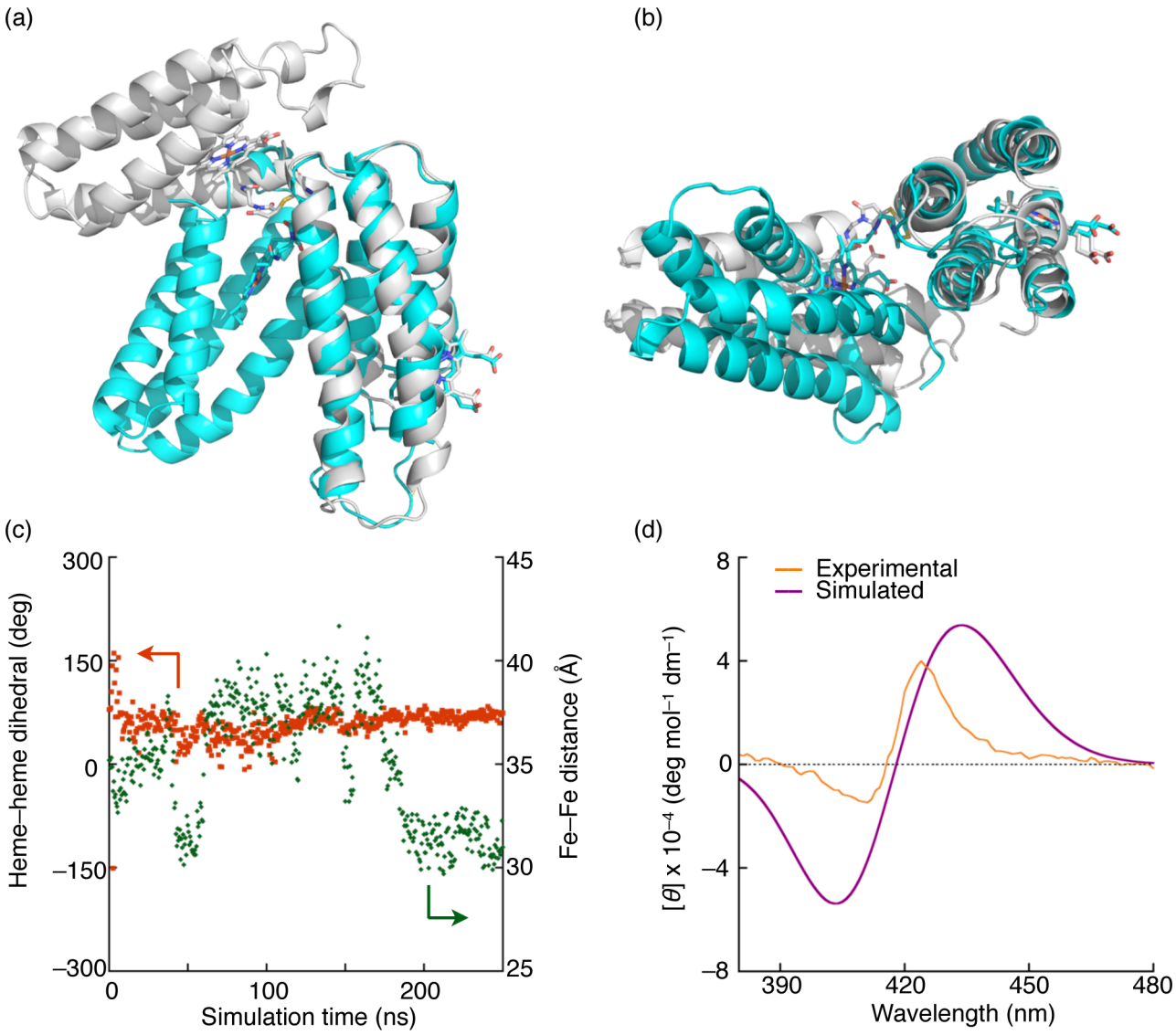

Figure S4. Dimer model C. The initial and MD-relaxed structures are shown in gray and cyan, respectively. The two structures are superimposed by Cα carbons of **1**-N80C with native heme. (a) Top view. (b) Side view. (c) The plots of important structural factors, heme–heme dihedral angles (red) and Fe–Fe distances (green), of the dimer model against the simulation time. (d) Simulated CD spectrum based on the model C (purple) and experimental CD spectrum (orange).

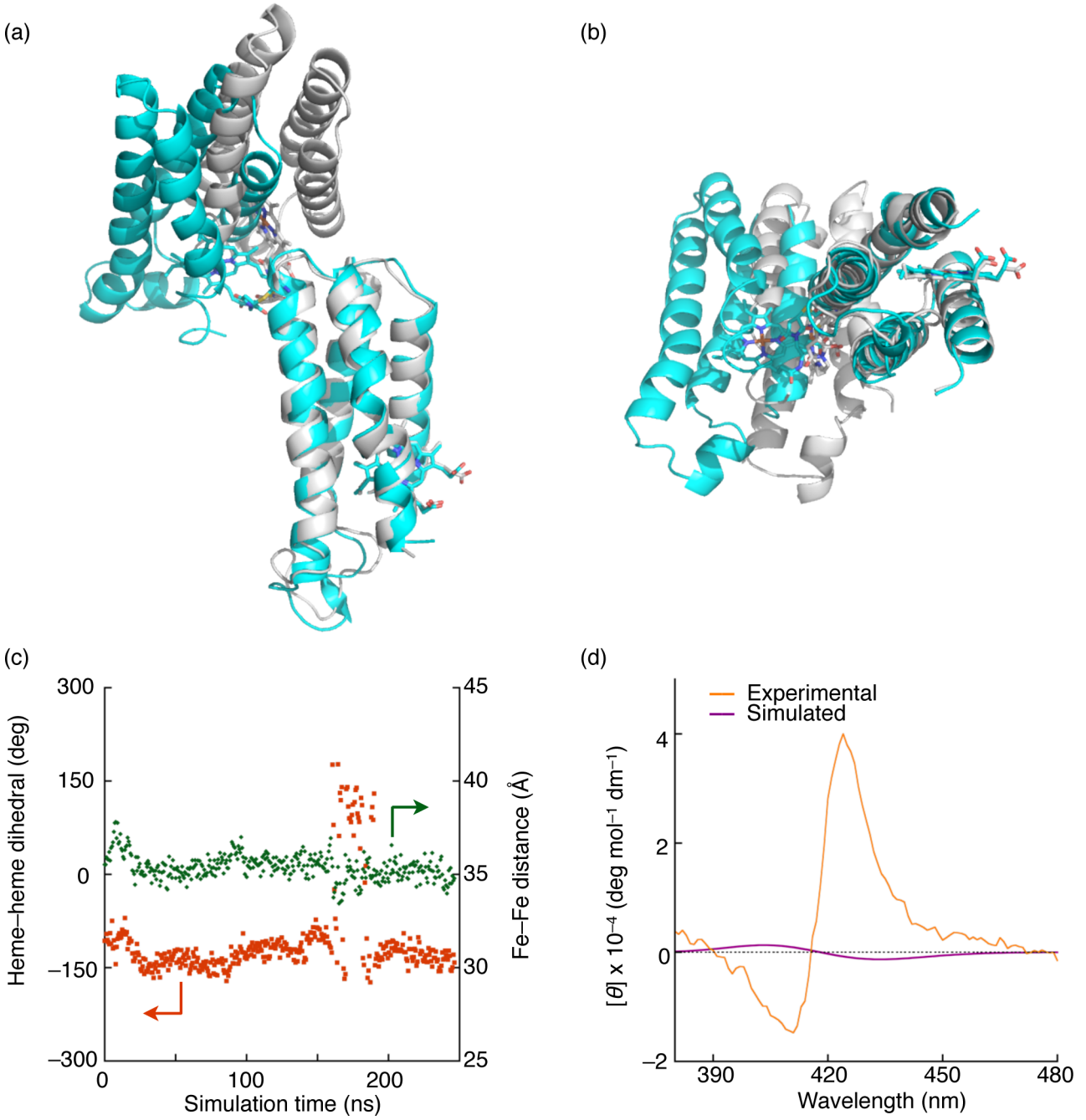

Figure S5. Dimer model D. The initial and MD-relaxed structures are shown in gray and cyan, respectively. The two structures are superimposed by Cα carbons of **1**-N80C with native heme. (a) Top view. (b) Side view. (c) The plots of important structural factors, heme–heme dihedral angles (red) and Fe–Fe distances (green), of the dimer model against the simulation time. (d) Simulated CD spectrum based on the model D (purple) and experimental CD spectrum (orange).

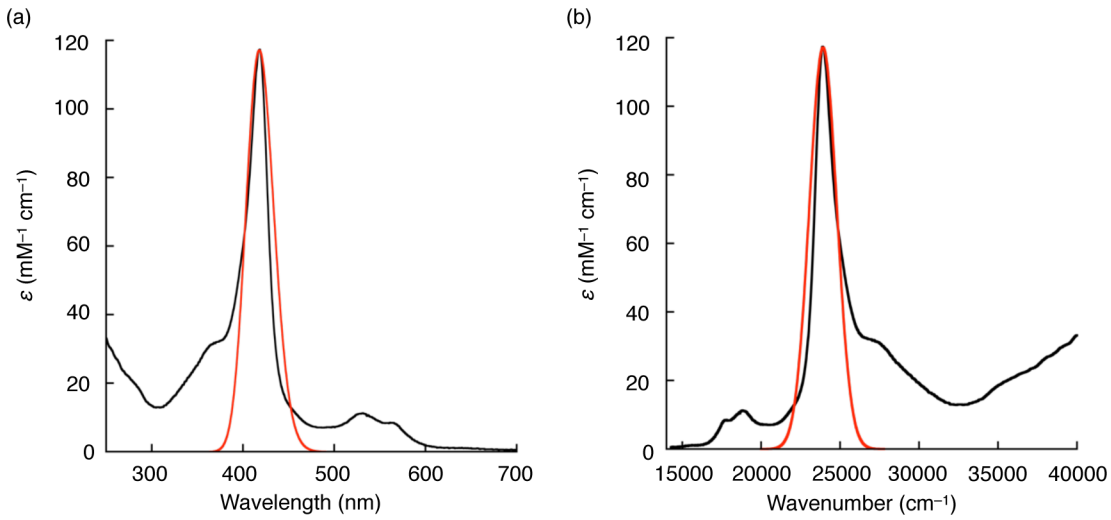

Figure S6. UV-vis absorption spectrum of the **1**-N80C assembly (black) and the fitting peak for the Soret band produced by the Gauss function (red): $\varepsilon(\sigma) = \varepsilon_{max} \exp(-(\sigma - \sigma_{max}^2)/\Delta\sigma^2)$, where ε is extinction coefficient, ε_{max} is ε at the peak top, σ is wavenumber, σ_{max} is σ at the peak top and $\Delta\sigma$ is the half-width of the wavenumber giving ε_{max}/e. (a) Extinction coefficient vs. wavelength. (b) Extinction coefficient vs. wavenumber.

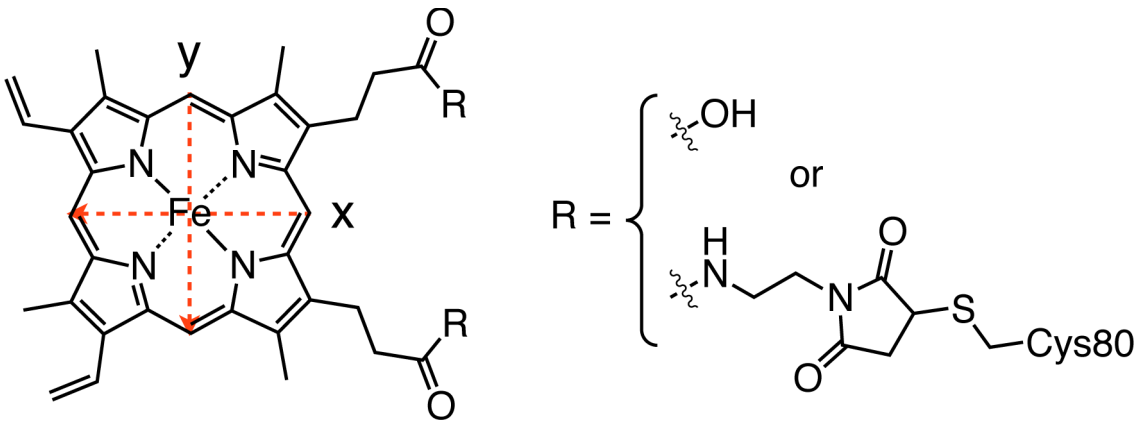

Figure S7. Polar coordinates used for simulation of CD spectra in the dimer model.

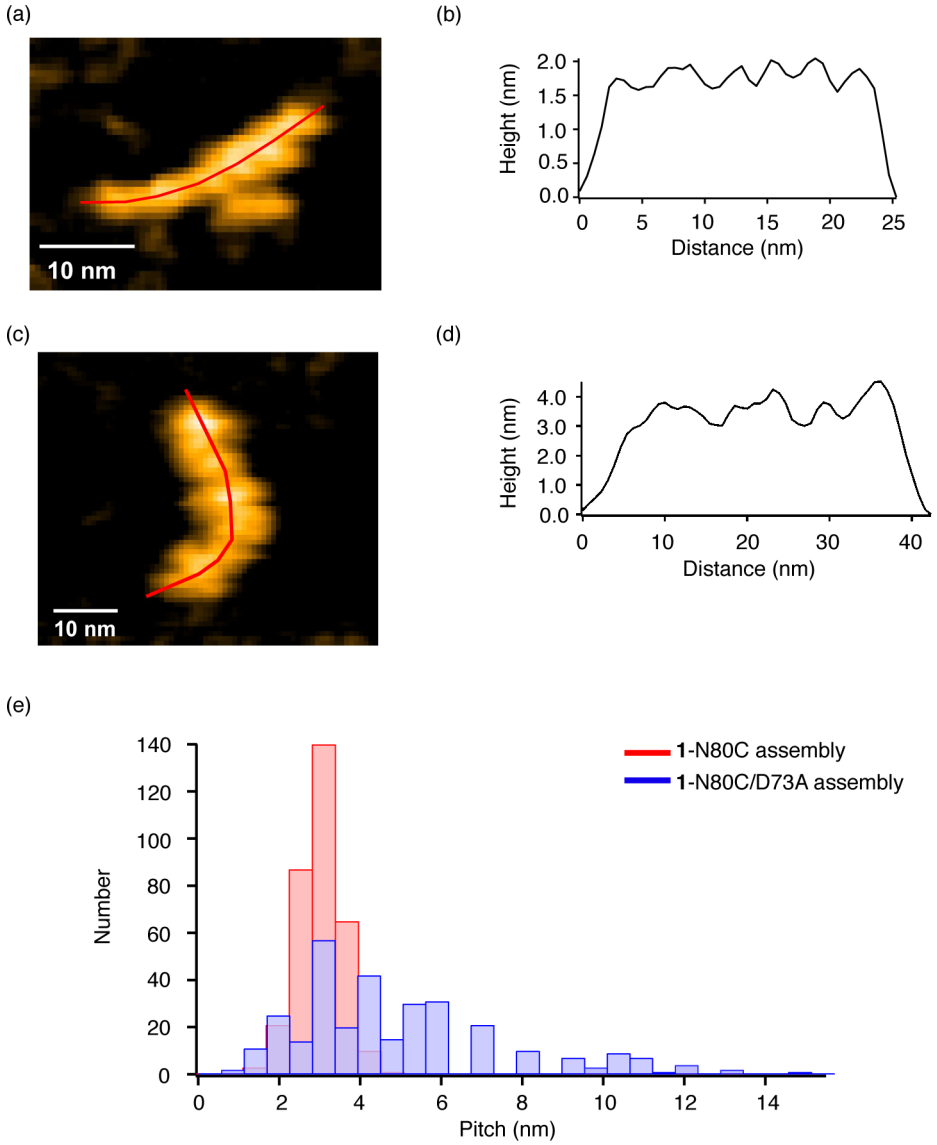

Figure S8. (a) Representative high-speed AFM image of the **1**-N80C assembly on an APTES-treated mica substrate. (b) Height profile along a red line in the image (a). (c) Representative high-speed AFM image of the **1**-N80C/D73A assembly on an APTES-treated mica substrate. (d) Height profile along a red line in the image (c). (e) Histograms of pitches from the height profiles for **1**-N80C assembly (red) and **1**-N80C/D73A assembly (blue).

Table S1. Coordinates to determine dipole unit vectors and positions of Fe centers for CD calculation of the dimer model A.[a]

	heme 1			heme 2		
	x	y	z	x	y	z
μ_{x1}[b]	7.789	-5.469	-2.536	-12.356	8.884	5.578
μ_{x2}[c]	5.244	-9.458	2.279	-15.383	14.718	7.419
μ_{y1}[d]	4.043	-8.494	-2.234	-16.165	10.083	8.376
μ_{y2}[e]	8.988	-6.418	1.952	-11.465	13.576	4.931
Fe	6.451	-7.412	-0.192	-13.907	11.777	6.541

[a]The coordinates are shown in left-handed system. [b]Coordinate for origination of the dipole vector x. [c]Coordinate for terminal of the dipole vector x. [d]Coordinate for origination of the dipole vector y. [e]Coordinate for terminal of the dipole vector y.

Table S2. Coordinates to determine dipole unit vectors and positions of Fe centers for CD calculation of the dimer model B.[a]

	heme 1			heme 2		
	x	y	z	x	y	z
μ_{x1}[b]	9.500	16.096	8.489	-5.867	-8.107	-6.426
μ_{x2}[c]	11.536	19.100	14.138	-7.275	-2.883	-2.195
μ_{y1}[d]	13.806	16.767	10.545	-5.237	-3.277	-6.500
μ_{y2}[e]	7.247	18.530	11.987	-7.897	-7.719	-2.017
Fe	10.465	17.596	11.282	-6.682	-5.523	-4.336

[a]The coordinates are shown in left-handed system. [b]Coordinate for origination of the dipole vector x. [c]Coordinate for terminal of the dipole vector x. [d]Coordinate for origination of the dipole vector y. [e]Coordinate for terminal of the dipole vector y.

Table S3. Coordinates to determine dipole unit vectors and positions of Fe centers for CD calculation of the dimer model C.[a]

	heme 1			heme 2		
	x	y	z	x	y	z
μ_{x1}[b]	12.886	5.361	7.171	-6.128	-3.933	-3.864
μ_{x2}[c]	19.464	4.692	6.571	-6.667	-4.188	2.745
μ_{y1}[d]	16.116	7.258	4.316	-5.307	-7.356	-0.634
μ_{y2}[e]	16.165	2.768	9.455	-6.944	-0.677	-0.497
Fe	16.134	4.957	6.843	-6.052	-3.926	-0.569

[a]The coordinates are shown in left-handed system. [b]Coordinate for origination of the dipole vector x. [c]Coordinate for terminal of the dipole vector x. [d]Coordinate for origination of the dipole vector y. [e]Coordinate for terminal of the dipole vector y.

Table S4. Coordinates to determine dipole unit vectors and positions of Fe centers for CD calculation of the dimer model D.[a]

	heme 1			heme 2		
	x	y	z	x	y	z
μ_{x1}[b]	45.300	56.734	55.367	78.713	61.116	58.823
μ_{x2}[c]	49.055	61.247	58.744	84.545	64.136	60.208
μ_{y1}[d]	46.247	57.416	60.037	82.763	59.662	60.895
μ_{y2}[e]	47.598	60.782	54.199	80.739	65.343	57.580
Fe	47.148	58.987	56.992	81.674	62.578	59.349

[a]The coordinates are shown in left-handed system. [b]Coordinate for origination of the dipole vector x. [c]Coordinate for terminal of the dipole vector x. [d]Coordinate for origination of the dipole vector y. [e]Coordinate for terminal of the dipole vector y.

Captions for Supporting Online Movies.

Movie S1. Representative high-speed AFM images for **1**-N80C assembly. Scan area: 30 × 17 nm^2 (120 × 60 $pixels^2$). Frame rate: 10 fps.

Movie S2. Representative high-speed AFM images for **1**-N80C assembly. Scan area: 200 × 200 nm^2 (180 × 150 $pixels^2$). Frame rate: 1 fps.

References

S1. Kitagishi, H.; Kakikura, Y.; Yamaguchi, H.; Oohora, K.; Harada, A.; Hayashi, T. *Angew. Chem., Int. Ed.* **2009**, *48*, 1271–1274.

S2. Kitagishi, H.; Oohora, K.; Yamaguchi, H.; Sato, H.; Matsuo, T.; Harada, A.; Hayashi, T. *J. Am. Chem. Soc.* **2007**, *129*, 10326–10327.

S3. (a) Ando, T.; Kodera, N.; Takai, E.; Maruyama, D.; Saito, K.; Toda, A. *Proc. Natl Acad. Sci. USA* **2001**, *98*, 12468−12472. (b) Ando, T.; Uchihashi, T.; Fukuma, T. *Prog. Surf. Sci.* **2008**, *83*, 337 −437.

S4. Wendel, M.; Lorenz, H.; Kottthaus, J. P. *Appl. Phys. Lett.* **1995**, *67*, 3732–3734.

S5. Krieger, E.; Darden, T.; Nabuurs, S.; Finkelstein, A.; Vriend, G. *Proteins* **2004**, *57*, 678–683.

S6. Duan, Y.; Wu, C.; Chowdhury, S.; Lee, M. C.; Xiong, G.; Zhang, W.; Yang, R.; Cieplak, P.; Luo, R.; Lee, T.; Caldwell, J.; Wang, J.; Kollman, P. *J. Comput. Chem.* **2003**, *24*, 1999–2012.

S7. Wang, J.; Wolf, R. M.; Caldwell, J. W.; Kollman, P. A.; Case, D. A. *J. Comput. Chem.* **2004**, *25*, 1157–1174.

S8. Jakalian, A.; Jack, D. B.; Bayly, C. I. *J. Comput. Chem.* **2002**, *23*, 1623–1641.

S9. Pescitelli, G.; Gabriel, S.; Wang, Y.; Fleischhauer, J.; Woody, R.W.; Berova, N. *J. Am. Chem. Soc.* **2003**, *125*, 7613–7628.

S10. Yamamura, T.; Mori, T.; Tsuda, Y.; Taguchi, T.; Josha, N. *J. Phys. Chem. A* **2007**, *111*, 2128–2138.